1.1 Introduction

Nanoparticles (NPs) have been extensively used as catalysts owing to their high surface area and thereby plenty of surface active sites. Interaction of reagents and substrate on the surface of nanoparticles having different active sites catalyzes the reaction. The nature of active sites and their density are dependent on the size, shape and composition of nanocatalysts [Cao *et al*. (2016)]. Higher catalytic activity can be obtained by altering the nature and increasing the density of active sites. Thus, modifications in anisotropic shapes offer different densities of surfaces, edges and corners in nanoparticles [Jing *et al.* (2014), Tran and Lu (2011)]. Atoms in corners and edges possess low coordination and can lead to better interaction with the substrate and other reacting species for catalysis. With the change in the size of nanoparticles, surface to volume ratio changes, and thereby providing active surface area for the catalysis [Cao *et al*. (2016)]. Synthesis of bimetallic nanoparticles by varying the composition of two metals not only reduces the cost of nanomaterial but shows synergistic effect in catalytic applications [Wu *et al*. (2012), Zhang *et al*. (2011a), Yin *et al*. (2011)].

Nanoparticles, owing to high surface energies, tend to get agglomerated resulting in enhanced particle sizes with lower surface area. Lower surface area means lesser number of surface active sites in the catalyst. Stabilizers such as surfactants or polymers are frequently used to protect nanoparticles surfaces against aggregation. Other approach to circumvent this problem is by adsorbing these NPs on large surface area but low density insoluble solid support such as metal oxides, zeolites, carbon based materials etc. The support material needs to be relatively inert otherwise it modifies chemical and adsorption properties of the catalyst. They can also affect the catalysis by tuning the electron density of NPs or by altering acidity/basicity to the medium.

Transition metals, specifically precious noble metals such as Pt, Pd, Rh, Ru, Au, Ag etc. are commonly used as heterogeneous catalysts in majority of chemical reactions [Haruta (2002)]. One of the primary reasons for this is the variable oxidation states offered by them. They also possess good adsorption properties essential for heterogeneous catalysis. Thus, transition metals particles act as electron conduits for the reactants adsorbed on the surface of the catalyst. While one of the reactants is reduced, the other one gets oxidized. In the process, the catalyst needs to get reduced and oxidized, making use of different oxidation states available and thereby for enabling electron transfer between the reactants. One of the first couple of examples of nanoparticles as catalyst relate to Ag nanoparticles in photography as well as Pt utilized in the decomposition of hydrogen peroxide (H_2O_2) [Astruc (2008)]. Following these, noble metal nanoparticles have been employed as catalysts for many organic reactions such as carbon-carbon coupling in Suzuki, Heck and Stille coupling reactions, hydrogenation, dehydrogenation reaction, oxidation, etc. [Hutchings (2013)].

Noble metals such as Au, Ag and Cu also possess good visible range optical properties which can be regulated by controlling the shape and size of NPs. Interaction of these metal NPs with visible light results in the localized surface plasmon resonance (LSPR), which is very sensitive to the size and shape of the NPs [Reguera *et al.* (2017), Potara *et al.* (2011), Murphy *et al.* (2005)]. The excitation involved in LSPR leads to the formation of energetic electrons on NPs having life time of a few femtoseconds. It has been reported that such electrons generated on NPs can drive photocatalytic transformations. These photocatalytic reactions represent a new family of chemical transformations which are electron driven. Such photocatalytic processes are different from those of phonon driven thermal reactions [Linic *et al.* (2013)]. Mainly two types of plasmonic metal induced

photocatalysts are used. These refer to plasmonic metal/semiconductor and direct plasmonic photocatalysts [Linic *et al.* (2011)]. Photocatalytic reactions occur at lower temperatures ensuring better catalyst stability and enhanced product selectivity [Linic *et al.* (2013)].

This thesis concentrates on investigating the catalytic properties of transition metals with good visible light LSPR absorbance. For such noble metal nanoparticles both thermal as well as plasmonic photocatalytic properties are of great interest. Reductive as well oxidative catalytic properties of these nanoparticles have been studied here. The next few sections introduce the basic concepts needed for presenting the detailed objectives of this thesis.

1.2 Catalysis

Catalysis is the increase in the rate of a chemical reaction due to the participation of an additional material called as catalysts. Catalyst is responsible for accelerating a selected chemical reaction, with lower activation energy, without being consumed itself as shown in Figure 1.1. The lower activation energies achieved, due to formation of new alternative pathways in reaction by the use of catalyst. Catalyst can facilitate adsorption, diffusion, and chemical rearrangements of reactants followed by desorption of the reaction products.

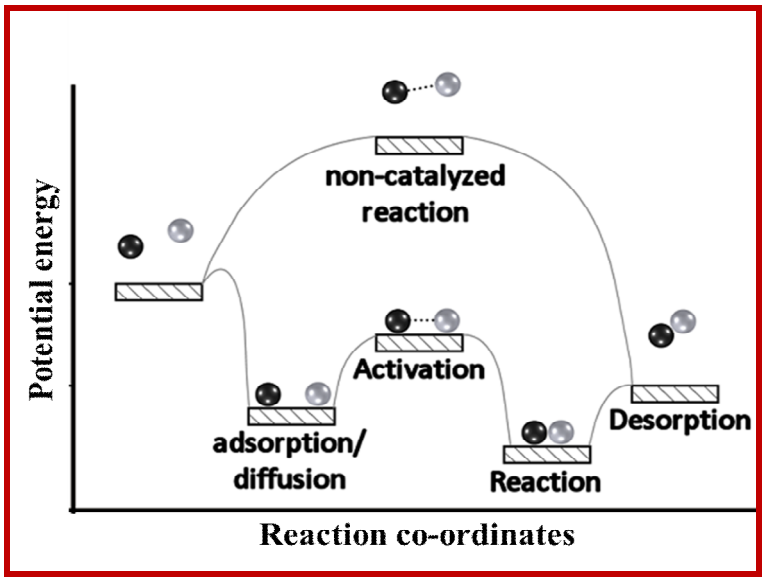

Figure 1.1 Potential energy diagrams for catalyzed and non-catalyzed reaction.

1.2.1 Homogeneous catalysis

Homogeneous catalytic processes contribute around 20 % in chemical industries [Whitby (2015)]. Its significance is increasing rapidly mainly in pharmaceutical and polymer industries. In homogeneous catalysis the catalyst and reactants are in the same phase. In this process, catalyst provides an alternative reaction pathway having lower activation energy. In homogeneous catalysis, the catalyst is more active with better selectivity. Some of the common homogeneous catalysts are HF, H_2SO_4, metal ions (Mn^{+2}, Cu^{2+}, etc.) as well as organometallic complexes, macrocyclic compounds and large enzyme molecules [Chadwick *et al.* (2011), Whyman *et al.* (2005)]. Some of the drawbacks of homogeneous catalysts are as follows:

1) The stability of homogeneous catalyst is selective in mild conditions. This limits their applicability.

2) These catalysts are molecularly dispersed in the same state as those of reactant, product and solvent. Therefore, recovery of catalyst in this process is not only difficult, but cost effective.

1.2.2 Heterogeneous catalysis

Contribution of heterogeneous catalytic processes in chemical industries is significantly greater than that of homogeneous catalytic processes. Majority of heterogeneous catalysts are in solid phase on which substrates in liquid or gas reacts. Thus, heterogeneous catalysis occurs at the interface of phases [Whitby (2015)]. Faraday in 1833 first suggested the theory of heterogeneous catalysis. This is based on the adsorption phenomenon. Transition metals and metal oxides are the common examples of heterogeneous catalysts. Heterogeneous catalyst provides an alternative reaction path which has lower activation energy, depending upon the activity of catalyst. The drawback of heterogeneous catalysis is given below:

1. These catalysts are less selective due to phase difference.
2. As this is completely dependent on the extent of adsorption, once the reactants adsorbed, the reaction depends on desorption of product.

The general mechanism of heterogeneous catalysis is shown in Figure 1.2. In the first step reactants ‘A’ and ‘B’ adsorbs on to the catalyst surface. The adsorbed reactants adjacent to each other forms an activated complex ‘AB*’. This activated complex reacts to produce product ‘P’ which desorbs from the surface of catalyst. This regenerated catalyst surface is further available for next catalytic cycle.

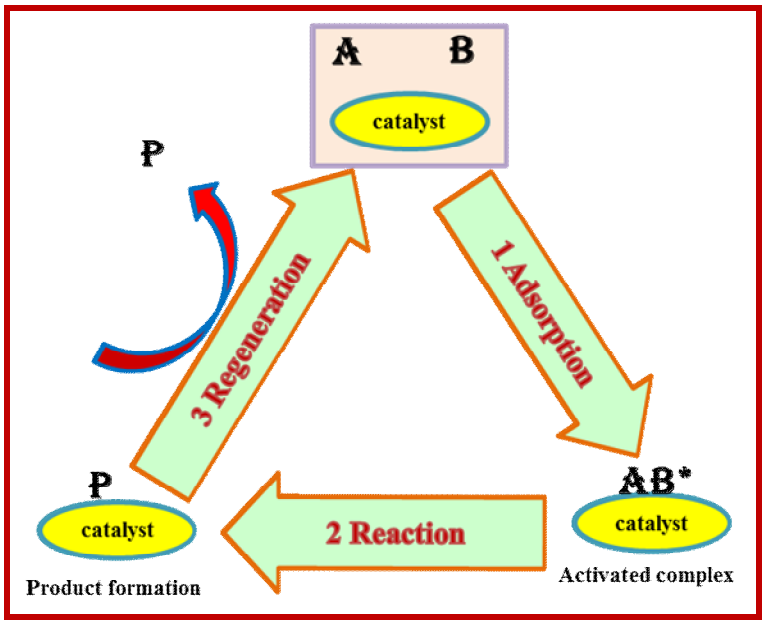

Figure 1.2 General mechanism of heterogeneous catalysis.

Depending upon the interaction of reactants with the catalyst surface three types of heterogeneous mechanisms are proposed. These are Langmuir-Hinshelwood, Eley-Rideal and Mars-Van Krevelen.

1.2.2.1 Mechanisms involved in heterogeneous catalysis

Langmuir-Hinshelwood Mechanism

Langmuir-Hinshelwood mechanism of heterogeneous catalysis involves following steps which are graphically shown in Figure 1.3.

1. Both the reactant molecules A and B adsorb on to the surface of catalyst.
2. Afterwards, surface diffusion of the adsorbed substrates on the catalyst surface results in better interaction and once the molecules are adjacent to each other they react to form an activated complex ‘AB’.

3. This activated complex immediately starts decomposing with the formation of product 'P'. As soon as product is desorbed from the catalyst surface, regeneration of catalyst active site takes place which again gets involved in second process. Rate of adsorption of reactant molecules is comparatively slower than desorption of product. The slower adsorption step is rate determining. Higher reaction rates are observed when the stoichiometric amounts of both reactants are adsorbed on the catalyst surface.

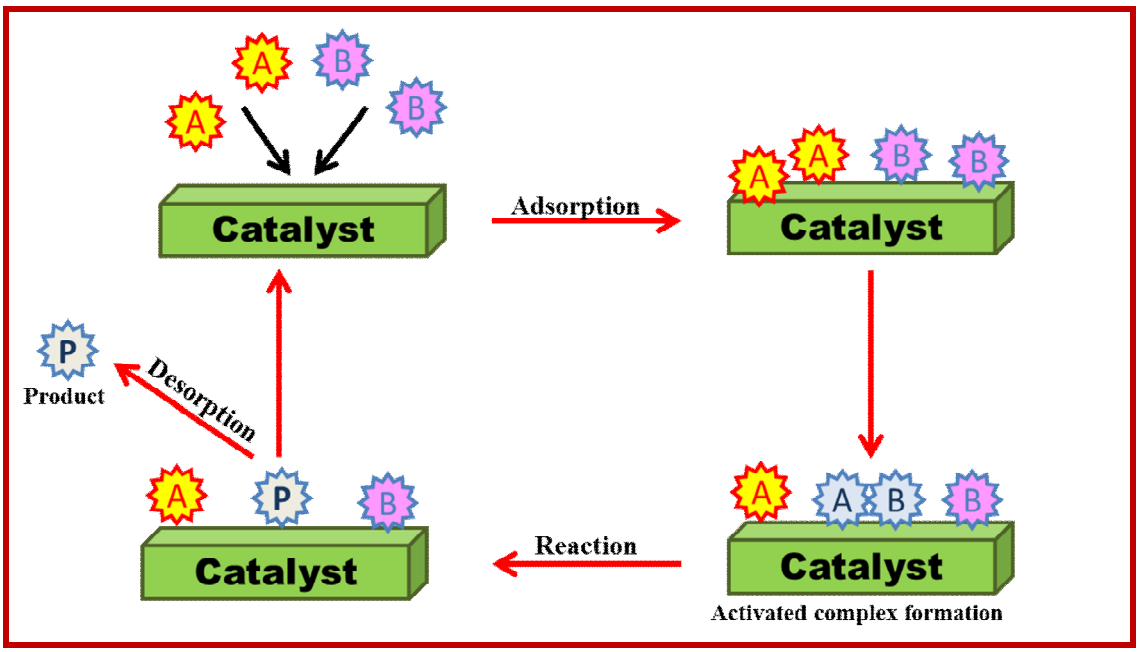

Figure 1.3 Schematic of Langmuir Hinshelwood mechanism for heterogeneous catalysis.

Eley-Rideal mechanism

The schematic of the Eley-Rideal (ER) mechanism is given in Figure 1.4. In this process the adsorption of only one reactant on to the surface of catalyst takes place. As shown in Figure 1.4 reactant B is adsorbed on the surface of catalyst. The second reactant 'A' remains in the adsorptive and directly interacts with the adsorbed molecule 'B' for the

formation of product 'P'. The product formed then desorbs from the surface of the catalyst. This produces a vacant active site on the catalyst available for further adsorption and reaction. At higher concentration of reactants higher reaction rates will be observed. In this case, the adsorbed reactant will occupy maximum surface of the catalyst and the other reactant will be available in the adsorptive for interaction with the adsorbed ones.

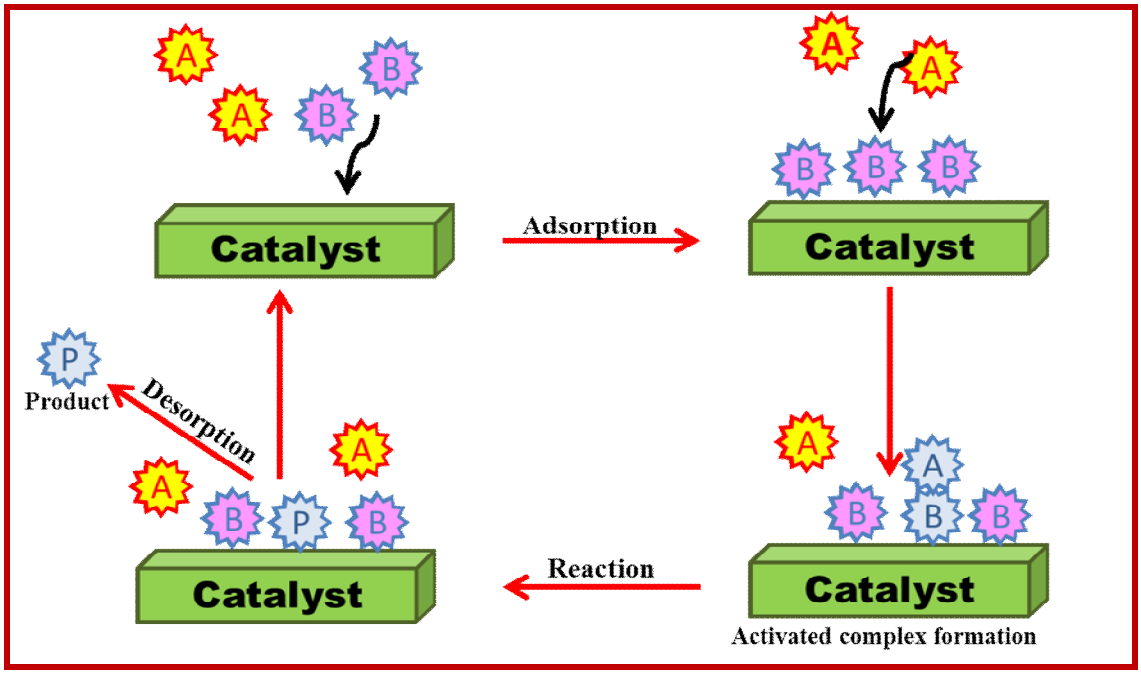

Figure 1.4 Schematic of Eley-Rideal mechanism for heterogeneous catalysis.

Mars-Van Krevelen mechanism

Third mechanism of heterogeneous catalysis is explained by Mars-Van Krevelen (MVK). The MVK mechanism appears nearly similar to the ER mechanism; it is shown schematically in Figure 1.5. As discussed above in ER mechanism one of the reactant (1) gets adsorbed on to the surface of catalyst and the second reactant (2) present in the reaction mixture directly reacts with adsorbed reactant (1) to form the product. In MVK

reaction one of the reactant (1a) gets adsorbed on to the surface of catalyst and forms an oxide layer. Therefore, in contrast to ER mechanism, the occurrence of MVK reaction requires prior transformation of adsorbed reactant into the surface oxide phase. This results in the formation of a thin surface oxide layer on catalyst surface by forming a chemical bond with it. Then the other reactant molecules (1b) present in gaseous or liquid phase directly reacts with the atom of the chemically bonded reactant on the catalyst surfaces.

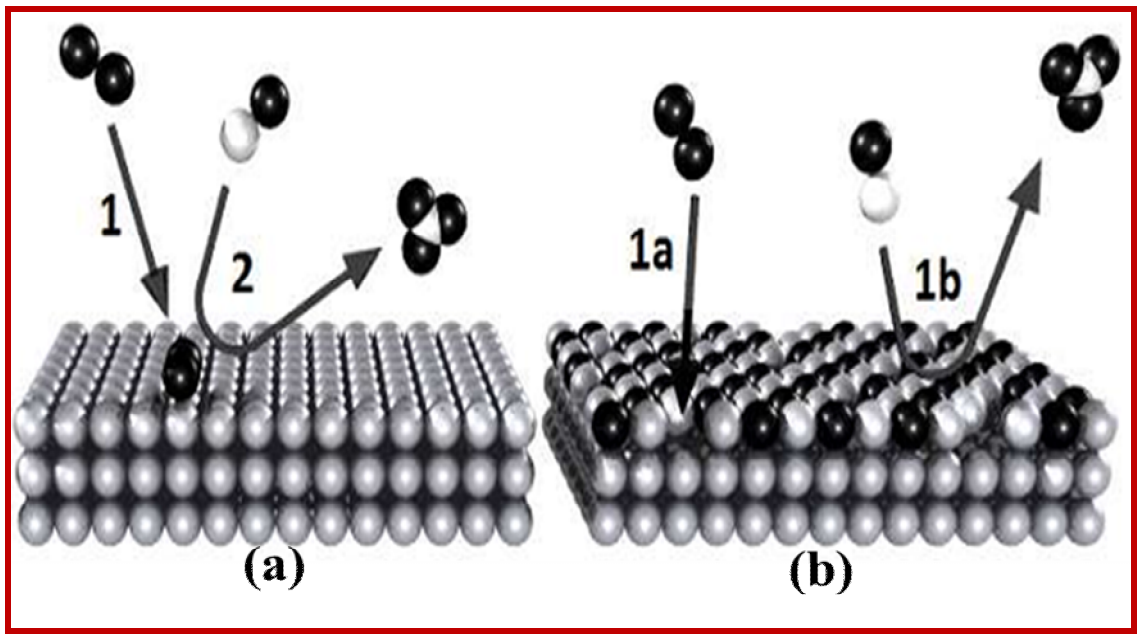

Figure 1.5 Comparison of Eley-Rideal (a) and Mars-Van Krevelen (b) mechanism for heterogeneous catalysis.

1.3 Nanocatalysis

Owing to some of the drawbacks in both homogeneous and heterogeneous catalysts, new catalytic systems are needed to overcome the limitations associated with both types. The systems should allow all the catalytic active sites to be effectively accessible (by providing good catalytic activity, selectivity, and yield), and make possible easy catalyst

separation (provide stable catalyst, catalyst recovery and catalyst reuse). Nanocatalysts could meet the need of such new catalytic systems.

Currently, nanoparticles are increasingly substituting conventional heterogeneous catalysts [Ozin *et al.* (2009)]. Nanoparticles have higher surface area and increased exposed active sites. They provide improved contact areas with reactants and are catalytically more active than conventional heterogeneous catalysts. Variation in shape and composition of nanoparticles leads to formation of nanocatalysts with different types of catalytic sites. Such site specificity means that these nanocatalysts also display more selectivity with respect to their catalytic activity for related reactions. Thus, from the point of view of increased activity and selectivity nanocatalysts have properties akin to those of homogeneous catalysts. On the other hand, nanocatalysts can be easily separated from the reaction mixtures and therefore are heterogeneous catalysts. Furthermore, adsorption of reactant(s) on to the nanocatalyst is a necessary precondition for any nanocatalyzed reaction. This is again characteristic of a heterogeneous catalytic process. Therefore, nanocatalysts can be improved by tailoring the chemical and physical properties of the nanomaterials by various synthetic methods. For example, nanocatalysts with better activity, stability, and selectivity can be designed and synthesized by controlling their size, shape, and composition [Astruc (2008), Ishida and Haruta (2007), Hashmi and Hutchings (2006)].

As mentioned above, the activity and selectivity of nanocatalyst is size, shape and composition dependent. Size, shape and composition changes the chemical and structural parameters of the nanocatalyst which affects its catalytic activity and selectivity. To study the size effect of catalyst, metal nanoparticles with the same shape but different sizes are applied in a reaction. The influence of nanoparticle size on catalytic activity and selectivity

can thus be determined. As all chemical processes occur on surface of catalysts, in case of bimetallic or alloy it is essential to correlate the surface composition and structure of nanocatalysts with their catalytic performance. Effect of change in size, shape and composition of nanocatalyst on catalysis is discussed in details in the following sub sections.

1.3.1 Effect of size on catalytic properties

Nanoparticle catalysts as compared with their bulk counterparts, commonly offers much higher surface-to-volume ratio. More significantly, prominent changes in the electronic states and coordination environment of the surface atoms of a catalyst nanoparticle might be possible when its size decreases typically to a certain nano-regime. Therefore, change in size of nanoparticles affects coordination environment, electronic state and adsorption energy of the reactant molecules.

1.3.1.1 Size dependent coordination environment

The effect of atoms at corners and edges of nanoparticles becomes dominant with decreasing the size of nanoparticles [Hvolbaek *et al*. (2007), Che and Bennett (1989)]. Cao *et al*. (2016) summarized a relation between surface metal atoms with different coordination numbers of cuboctahedral and cubic geometry of nanoparticles with overall size of the nanoparticles [Hvolbaek *et al*. (2007), Che and Bennett (1989)]. They concluded that the coordination numbers 9, 7 and 4 of a cuboctahedral nanoparticle and 8, 6 and 3 in a cubic nanoparticle exhibits strong dependence on the size of the nanoparticle. Such strong correlation of size-dependent catalytic performance (for a particular nanocatalyst shape) was also reported by Tao *et al.* (2010) for room temperature CO oxidation reaction. For instance, in Pt nanoparticles with a size of about 2.2 nm, the Pt atoms (CN = 7) at the edge

of triangular nanoclusters are active for CO oxidation even at room temperature. However, Pt atoms with CN of 9 on the terrace of Pt (111) are not active for CO oxidation at room temperature [Tao *et al.* (2010)].

1.3.1.2 Size dependent electronic state

The electronic structure of metal nanoparticles of 1 - 2 nm is like that of a molecule. Thus, Au nanoparticles smaller than 1 nm, are more molecular than metallic [Cleveland *et al.* (1997). Thus, molecule-like electronic states of metal nanoparticles of 1 - 2 nm exhibits inherently different catalytic performance in contrast to a nanoparticle with a larger size [Cao *et al.* (2016)]. This was experimentally demonstrated for the first time, in CO oxidation on Au nanocluster with thickness of three atomic layers supported on TiO_2 [Chen and Goodman (2008), Chen and Goodman (2004), Valden *et al.* (1998)]. Analysis of Au L_{III} X-ray absorption near-edge spectroscopy (XANES) white lines by these authors revealed that supported Au nanoparticles with different sizes have different average coordination numbers. Thus Au nanoparticle of 3 nm has average CN = 9.5, similarly the nanoparticles of 1 nm have an average CN = 6, while nanoparticles of 0.5–1 nm have CN = 3.6. This shows that smaller Au nanoparticles have a size-dependent electronic environment [Walsh *et al.*(2012), Van Bokhoven and Miller (2007), Van Bokhoven *et al.* (2006), Janssens *et al.* (2006), Miller *et al.* (2006), Schwartz *et al.* (2004)].

1.3.1.3 Size dependent adsorption energy

Adsorption is a primary step in heterogeneous catalysis. Size dependent adsorption energies of reactants on catalyst surfaces with different coordination numbers have also been suggested in literature. It has been argued in literature that the adsorption energy is dependent on the coordination environment of metal nanoparticles [Somorjai and Li (2010),

Somorjai (1981)]. Usually, catalyst atom(s) with low coordination number (CN) exhibits stronger adsorption for a given molecule than those catalyst atoms with higher coordination number [Somorjai and Li (2010), Somorjai (1981)]. For example, adsorption energy of adsorbates including ●O_2, ●OH, ●OOH, ●O, ●H_2O, and ●H_2O_2 on Pt nanocatalyst decrease linearly with increase in coordination number from 3 to 9 [Calle-Vallejo *et al.* (2014)]. Similar linear relationships between adsorption energy and coordination number have been reported for other transition metal catalysts such as Co, Ni, Cu, Rh, Pd, Ag, Ir and Au [Calle-Vallejo *et al.* (2015)].

1.3.2 Effect of shape on catalytic properties

The representative shapes of metal nanoparticles based on dimensionality are shown in Figure 1.6. Spherical, pseudo-spherical, dodecahedral, tetrahedral, octahedral, cubic shape represents 0D nanoparticles. 1D morphology of nanoparticles includes nanotubes, nanorods or nanowires, nanocapsules, etc. [Lu *et al.* (2015), Zhang *et al*. (2014)].

Hexagonal, triangular, quadrangular plates or sheets, belts, rings, etc. fit in to the 2D shape NPs [Li *et al.* (2012)]. 3D morphologies of nanoparticles are complex such as nanoflowers, nanostars, polygonalnano frames etc. [Lv *et al.* (2015), Lin *et al*. (2012)]. Compared to simple isotropic morphologies of nanoparticles, novel anisotropic morphologies have unique physicochemical properties due to the different numbers of steps, edges and kink sites present on to the surface of catalyst in nanoscale regime. For example, polyhedral Au NPs with high-indexed facets are found to exhibit excellent optical and catalytic properties [Jing *et al*. (2014), Tran and Lu (2011)].

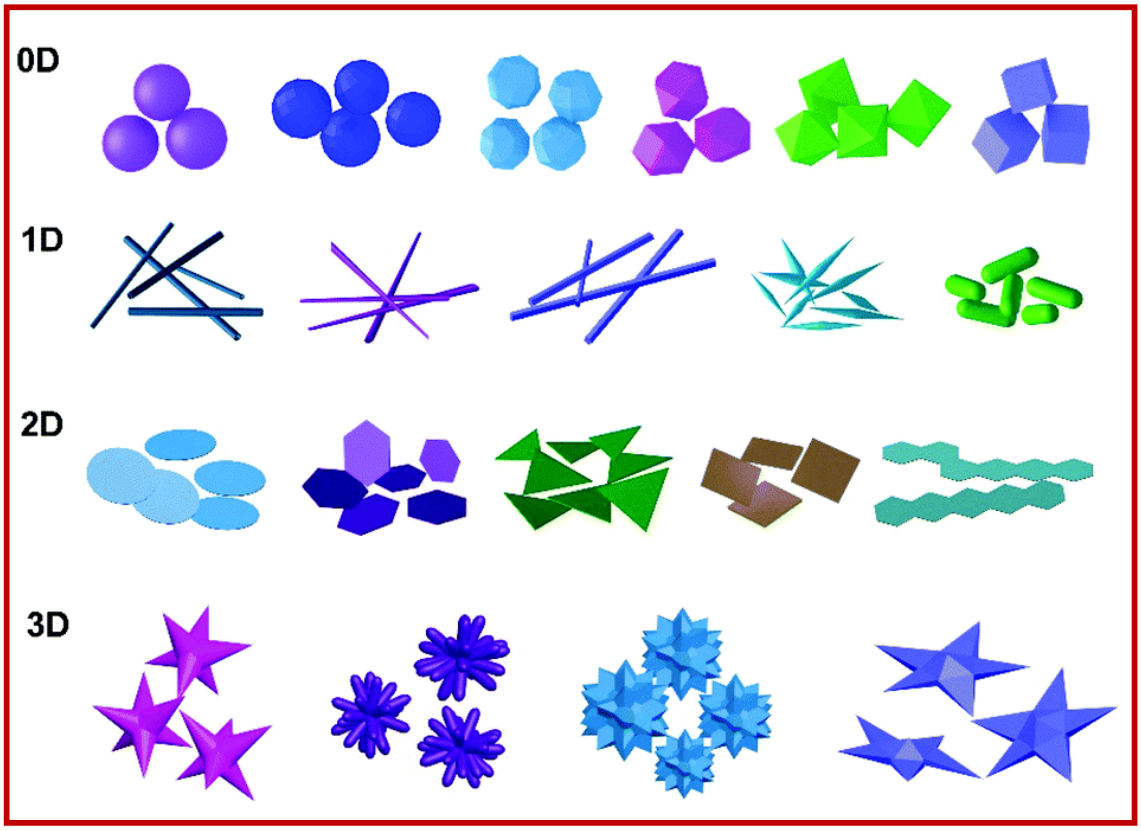

Figure 1.6 Different shapes of nanoparticles possible with respect to dimension in nano regime, 0D, 1D, 2D and 3D.

Gold rods with different ratios of length and width display different transverse and longitudinal plasmon bands. Preicel *et al.* (2016) have recently published a review on different types of anisotropic gold nanoparticles used in catalysis.

1.3.3 Composition effect

The research work in this thesis primarily deals with metal nanocatalysts; therefore, this section introduces the effect of composition on catalytic activity from the perspective of alloy and bimetallic nanoparticles only. Commonly, bimetallic nanoparticles can be categorized into alloy (ordered or random), intermetallics, Janus or core-shell structure

types. The type of bimetallic or alloy nanostructures formed depends on the synthesis methodology utilized (Figure 1.7).

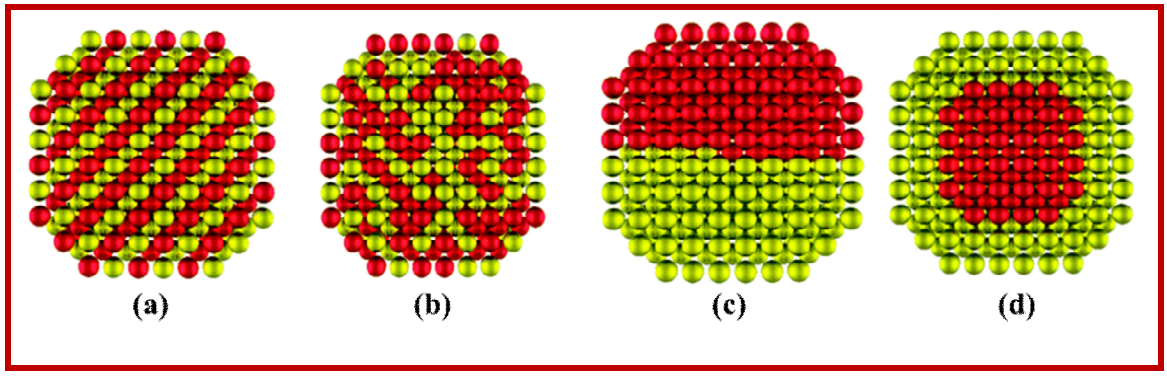

Figure 1.7 Different possibilities of bimetallic nanostructures observed. (a) Ordered alloy; (b) Random alloy (c) Janus-like; and (d) Core shell.

Catalytic activity of bimetallic nanomaterials is different from those of its component metals. Instead of being an average of the catalytic activities of its components, bimetallic nanoparticles may also exhibit synergistic catalytic properties. That is, the properties exhibited are not simply additives but exceed those of the individual component [Wu *et al*. (2012), Zhang *et al*. (2011a), Yin *et al*. (2011)]. Some examples of composition effect in catalytic reduction and oxidation reactions are discussed below.

Composition effect was studied by Lim and co-workers in catalytic activity of Pt-Y alloy for electrocatalytic oxygen reduction [Yoo *et al*. (2011)]. The addition of various amount of Y changes the electronic structure of Pt and thus modifies the binding energy of the oxygen-containing species. The maximum possible catalytic performance was achieved at a particular composition of Pt-Y alloy. Thus, the catalytic activity of Pt-Y alloy catalysts follows the trend of $Pt_{70}Y_{30}$ > $Pt_{78}Y_{22}$ > $Pt_{64}Y_{36}$ > $Pt_{86}Y_{14}$ > $Pt_{91}Y_{9}$ > Pt.

Sun and co-workers also demonstrated such composition-dependent catalytic activity of monodisperse CoPd nanoparticles for formic acid oxidation [Mazumder *et al.* (2012)]. Extensive use of BNPs have been reported in catalytic oxidation of glucose [Zhang *et al*. (2011b))], CO [Han *et al.* (2014)], benzyl alcohol [Deplanche *et al*. (2012)], and methanol [Fu *et al.* (2014), Duan *et al.* (2013)] oxygen reduction [Yamamoto *et al*. (2011), Watanabe *et al*. (1975)] propane dehydrogenation [Han *et al*. (2014)] hydrogenation of nitro-aromatic compounds [Wei *et al.* (2014), Xie *et al*. (2011)], electro-catalytic oxidation of methanol [Zhang *et al.* (2013), Luo *et al.* (2009), Bus *et al*. (2007), Zeng *et al.* (2006), Luo *et al.* (2006), Tada *et al*. (2002)] as well as in desulfurization of thiophene [Suo *et al.* (2011)].

Given the effect of size, shape and composition of metal nanoparticles on their catalytic properties, the next section discusses and gives a brief literature survey of various aspects of metal nanoparticle synthesis.

1.4 Synthesis of Nanoparticles

Producing metal nanoparticles of different size, shape, composition and morphologies require control over various aspects of their preparation protocols. Consequently, this sub-section introduces protocols for synthesis of mono/bimetallic nanoparticles to be used in the research work presented in this thesis. Nanoparticles are commonly synthesized by two main methodologies such as top-down and bottom-up approach. The top-down approach involves breaking down bulk materials into finer particles until nano-dimensions are reached. Top down method includes ball milling, laser ablation and etching [Russo *et al.* (2011)]. In the bottom-up approach, nanomaterials are formed by chemical reaction of atoms or molecule precursors. Bottom-up approach results

in better reproducibility. It is more economical and therefore, is used extensively for synthesis of new materials at nanometer length scale.

Generally, bottom-up methods such as chemical reduction, thermal decomposition, hydrothermal synthesis, microemulsion, sonochemical, electrochemical, microorganism and bacterial synthesis, etc. are employed for liquid phase synthesis of nanoparticle [Cabrera *et al.* (2008), Roh *et al*. (2006)]. Among them, majority of metal and bimetallic nanoparticle syntheses are based on chemical reduction or co-precipitation methods. In these methods, phase and size of the particles formed are affected by the concentration of metal ions, pH, solvent, reaction temperature [Khaleel (2004), Chastellain *et al.* (2004), Tronc *et al.* (1992), Tamaura *et al.* (1983)] and time of heating. Various precursors such as inorganic salts and metal complexes can be used for these chemical reduction based preparation techniques.

The first step in such synthesis involves the formation of reduced metal atoms, which then through random fluctuations form clusters of the second (or crystalline) phase. Some of these clusters may be larger than the critical size needed for stable nucleation. Although such clusters are supercritical they still have a very high surface areas and thereby surface energies. To reduce this, nanoparticles tend to grow or aggregate. This may result in the change of shape and size of the nanoparticles with time. To control the growth of particles within a certain nano regime, passivation, protection or stabilization of their surfaces is needed. Particle surface stabilization is, therefore, a fundamental requirement for liquid phase chemical reduction synthesis of mono or bimetallic nanoparticles.

1.4.1 Synthesis of monometallic Nanoparticles

Monometallic nanoparticles can be synthesized by different routes. Important parameters like temperature, reaction time, reactant concentration, the ratio of precursor to stabilizer all contribute greatly to the final size and shape of nanoparticles formed. The size of the nanoparticles increases with reaction time, as more number of atoms or molecules is added to the surface of nanoparticle. At higher temperatures, the reaction rate of solute in the solvent increases, producing larger nanoparticles. The concentration ratio of precursor to stabilizer also provides control over the particle size.

1.4.1.1 Chemical reduction

In chemical reduction method, hydrides (sodium borohydride, hydrazine), gases such as molecular hydrogen or carbon monoxide, or reagent like sodium citrate and alcohols are utilized as reducing agents. Phosphorous was the first reducing agent reported for synthesis of Au NPs, which was used by Faraday to reduce $AuCl^{4-}$ ions [Faraday (1857)]. Sodium citrate has also been a common reducing agent used for the formation of transition metal nanoparticles [Kumar *et al.* (2007), Harriman *et al.* (1987), Turkevich *et al.* (1951)]. Turkevitch *et al.* (1951) reported many important studies on the nucleation and growth of Au nanoparticles reduced by sodium citrate. One advantage of this method is that the citrate anion not only acts as a reducing agent but also as a stabilizer [Turkevich *et al.* (1951)]. With sodium citrate as reducing agent initially, oxidation of citrate occurs by formation of dicarboxyacetone. Further, it is involved in the reduction of auric salt to aurous salt and thereby leading to the formation of gold atom. Utilizing citrate, Ir and Pt nanoparticles have been synthesized [Harriman *et al.* (1987), Furlong *et al.* (1984)]. $NaBH_4$ or KBH_4 reduction agents have also been used for the synthesis of Au, Ag, Pt, Pd, and Cu

nanoparticles [Chechik and Crooks (2000) , Zhao *et al.* (1999), Zhao *et al.* (1998), Mayer and Mark (1997), Furlong *et al.* (1984)].

As copper is thermodynamically stable in its oxide form, it is difficult to get elemental copper in aqueous solution. Thus, limited number of reports has been published on formation of pure metallic copper nanoparticles. However, most of these recent strategies employ oxygen free environments and heavy molecular weight polymers as protecting agents. Therefore, copper nanoparticles in aqueous medium were reported in oxygen free atmosphere to prevent it from oxidation [Joshi *et al.* (1998)]. Likewise, Park *et al.* (2007) also reported polymer (PVP) stabilized copper nanoparticles which prevents it from oxidation and aggregation. Later aqueous medium synthesis of copper nanoparticles by alkaline hydrazine hydrate was reported [Singh *et al.* (2009)]. In contrast to the earlier preparation methods, here no external inert gas purging was required to ensure oxygen free atmosphere. Alkaline solution of hydrazine hydrate leads to in situ generation of N_2 gas which creates inert reaction atmosphere for proper reduction of copper salt to copper.

Much progress has been reported in the synthesis of shape-controlled NPs over the past decades [Long *et al.* (2014), Millstone *et al.* (2009)]. The next section describes briefly the salient features of liquid phase chemical synthesis of anisotropic nanoparticles by polyol process and by use of etchants.

1.4.1.2 Polyol method of reduction

Fivet *et al.* (1989a) originally established polyol synthesis. It is a simple and flexible route to form colloidal particles of metals (Ag, Au, Cu, Co, Ir, Ni, Pd, Pt, Ru) and their alloys (CoNi, FeNi) [Bonet *et al.* (1999), Toneguzzo *et al.* (1998), Fievet *et al.* (1989a), Fievet *et al.* (1989b), Viau *et al.* (1996)]. Commonly PVP is employed as a

stabilizer to prevent agglomeration of the nanoparticles. This involves the use of high boiling multivalent alcohols such as ethylene glycol, glycerol etc. which functions as the solvent as well as the reducing agent for the synthesis of metal nanoparticles [Ducamp-Sanguesa *et al.* (1992)]. The reduction kinetics depends on the precursor and heating conditions employed for the synthesis. For a given precursor, careful regulation of reaction temperature and time of heating can be used to control the nucleation and growth processes of nanocrystals. Wiley *et al.* (2005) reported the critical role of PVP in not only stabilizing the nanoparticles against aggregation and further growth, but also in determining the shapes of silver nanostructures formed [Sun and Xia (2002a), Sun and Xia (2002b)]. Significantly different strengths of interaction of PVP with different crystallographic facets of silver appears to be responsible for the anisotropic growth of silver [Wiley *et al.* (2005)] nanostructures obtained under these conditions [Wiley *et al.* (2005), Sun *et al.* (2002a)]. Murphy (2002) has reported the synthesis of silver nanocubes. Cao *et al.* (2003) could attain the synthesis of copper nanorods with higher yield, using a composite template of polyethylene glycol (PEG) and cetyltrimethylammonium bromide (CTAB). Park *et al.* (2007) synthesized monodisperse CuNPs by polyol method.

1.4.1.3 By utilizing etchants

In the synthesis of nanoparticles, the formed zero-valent species such as atoms, clusters, and nanocrystallites, can be oxidized back to the ionic form due to the presence of trace amount of etchants. This oxidation of zero-valent species on the surface of initially formed small super critical nuclei/nanoparticles alters the shape and distribution of anisotropic nanostructures obtained. Thus, trace amounts of salts such as NaCl, $Fe(NO)_3$, $CuCl_2$ and CuCl, have been found to act as etchants and influence the morphology of the

nanoparticles. Xia *et al.* (2009) have proposed that the etchant attacks and exposes particular facet(s) of the initial nanocrystal. Growth of the nanoparticle then preferentially occurs along the exposed facet(s) to a nanostructure of particular shape. For example, the synthesis of silver nanowires can be effectively achieved by salt-mediated method [Tang and Tsuji (2010)].

1.4.1.4 Green Synthesis

Green synthesis of nanomaterials involves nontoxic and natural materials like plant extract (leave, flower, bark, seed, peels etc.), fungi, bacteria, and enzyme. Green synthesis of nanoparticles has its own benefits; this method is ecofriendly and compatible for pharmaceutical and other biomedical applications. Noble metal (Au, Ag, Pt, etc.) and non-noble metal (Fe, Cu, ZnO, etc) are used in biomedical applications such as pharmaceutical, antibacterial, disease diagnostic, etc. Therefore use of green synthesis protocols are appeared to be an attractive alternative to traditional synthesis methods for producing nanoparticles. Shah et al discussed in detail, green synthesis protocols through biological entities and their potential applications [Shah *et al.* (2015)]. Green synthesis protocol is dependent on pH, reaction temperature, reaction time and the concentrations of reactants for synthesis [Shah *et al.* (2015)]. Synthesis of AuNPs are reported using glucose-starch as reducing and stabilizing agent and these are applied in bioelectrochemistry [Engelbrekt *et al.* (2009)]. Green synthesis of silver nanoparticles using starch as stabilizer is also reported [Singh *et al.* (2009)]. Another starch obtained from Sella and Mansoori rice is also utilized in stabilization of Silver nanoparticles [Singh *et al.* (2015)]. Synthesis of AgNPs was also reported by using white sugar in alkaline pH under sunlight [Meshram *et al.* (2013)].

1.4.2 Synthesis of bimetallic nanoparticles

A variety of bimetallic nanoparticles can be prepared by co-reduction, successive reduction and thermal decomposition protocols.

1.4.2.1 Co-reduction

It is the most common method for generating alloy or bimetallic A-B nanocrystals. In this method two metal ions in a solution are simultaneously subjected to chemical reduction. Synthesis of various bimetallic nanoparticles such as, Pd-Pt, Au-Pd, Pt- Rh, Pt-Ru, Pd-Ru, and Ag-Pd [Toshima *et al.* (1997), Yu *et al.* (1997), Silvert *et al.* (1996) Toshima *et al.* (1992), Toshima *et al.* (1991)] have been reported by this method. Various strong reducing agents mentioned earlier (in the sub-section on chemical reduction), such as hydrides etc, have also been successfully applied for preparing bimetallic nanoparticles. In this connection, it is relevant to mention that different tetraalkylammoniumhydrotriorganoborates ($NR_4(Bet_3H)$) have been used as a reducing agent for producing a wide variety of bimetallic nanoparticles in organic media [Bonnemann *et al.* (1998), Schmidt *et al.* (1997), Bonnemann *et al.* (1991)]. Co-reduction gives rise to a large number of bimetallic nanocrystals, where the final arrangement of metals can be tailored by varying different experimental parameters such as reduction potentials of metal ions, type of reducing agent, the nature of stabilizer and the reaction temperature. Generally, if the equilibrium phase diagram of the bimetallic system shows miscibility over a large composition range, then the possibility of co-reduction leading to formation of alloy nanoparticles is high. For instance, Ag-Au show almost complete miscibility and most co-reduction preparation protocols involving Ag and Au result in formation of their alloy nanoparticles. On the other hand, co-reduction in case of bimetallic

systems, which have significant miscibility gaps in their equilibrium phase diagrams, could result in various types of bimetallic systems. Thus, variations in polyol synthesis co-reduction parameters can facilitate the formation of micro phase-separated or core-shell or partial core-shell bimetallic nanostructures. For instance, the synthesis of these types of different Ag-Cu bimetallic nanostructures has been reported by the polyol route.

As mentioned above, co-reduction can also lead to the formation of nanoparticles with core-shell structures. The metal having higher reduction potential is easily reduced and forms the core [Toshima and Yonezawa (1998)]. The delayed reduction of the second metal means that it is reduce on the surface of the core through heterogeneous nucleation and thereby forms the shell. Formation of core-shell nanostructures by simultaneous reduction of $PdCl_2$ and H_2PtCl_6 in ethanol/water system in presence of PVP stabilizer is reported [Toshima *et al*. (1991)]. The Pd nanoparticles formed first having high reduction potential than Pt. Another factor that could influence the formation of core-shell nanostructures during a co-reduction synthesis protocol is the coordination ability of the stabilizer with the metal. If the stabilizer molecule forms a strong complex with one of the metal ions, then its reduction gets delayed in comparison to the other metal salt precursor, leading to formation core-shell particles [Toshima and Yonezawa (1998)].

1.4.2.2 Thermal decomposition

Another method of synthesis of bimetallic nanocrystals pertains to simultaneous thermal decomposition or thermolysis. It is effective for the synthesis of a variety of monometallic, bimetallic and metal-oxide nanocrystals. Conventionally, thermal decomposition has been favored for the metal precursors having relatively low reduction potentials and therefore, cannot be easily reduced chemically (e.g., Fe, Co, and Ni) [Puntes

et al. (2001), Park *et al*. (2000), Ely *et al.* (1999)]. In thermal decomposition, both the metals are linked to a coordination complex as separate parts. At higher temperatures the chelating ligands of coordination complex undergo decomposition. Rutledge *et al*. (2006), prepared first a bimetallic precursor, $Pt_3Fe_3(CO)_{15}$, by reacting $Fe(CO)_5$ with tris-(norbornylene)-platinum(0). In the presence of oleic acid (OA) and oleylamine (OLA), this preformed precursor ($Pt_3Fe_3(CO)_{15}$) was subjected to thermal decomposition in toluene. FePt nanocrystals were formed with an average diameter of 5.8 nm. Thanh et al. have also reported the synthesis of bimetallic magnetic nanocrystals by thermal decomposition of different precursors such as bimetallic carbonyl cluster anions such as $[FeCo_3(CO)_{12}]^{1-}$, $[Fe_3Pt_3(CO)_{15}]^{1-}$, $[FeNi_5(CO)_{13}]^{2-}$, and $[Fe_4Pt(CO)_{16}]^{2-}$ [Robinson *et al.* (2009)].

1.4.2.3 Successive reduction or seed mediated synthesis

In successive reduction, core shell structures are obtained by growing the second metal on the surface of metal seeds of first metal. Examples of core-shell structures resulting from the seed-mediated route include Au@ Ag [Tsuji *et al*. (2008), Yoo *et al*. (2009)], Ag@Au [Gao *et al.* (2012), Sanedrin *et al*. (2005)], Pd@Ag [Huang *et al*. (2011)], etc. Huang *et al*. (2011) synthesized Pd@Ag nanoplates through a seed-mediated approach, where Pd nanoplates were coated with Ag shells of various thicknesses. They also found that the LSPR positions could be readily adjusted across the visible region simply by adjusting the Ag (shell) thickness (e.g., with LSPR ranging from 477 - 971 nm). It should also be noted that, successive reduction method does not always lead to the formation of core-shell nanostructures. The formation of alloy structures or physical mixtures of the two metals have also been reported (owing to galvanic displacement and other reasons) by this method [Toshima and Yonezawa (1998)].

After this succinct description of liquid phase chemical synthesis of different types of metal nanoparticles, the next section turns to the discussion of catalytic properties of such nanostructures.

1.5 Stabilization of nanoparticles

The stability of nanoparticles against aggregation in a given solvent is in top priority from the view point of various applications. The forces acting between colloidal nanoparticles have been described by Derjaguin-Landau-Verwey-Overbeek (DLVO) theory. Two or more nearby placed particles within short interplanar distance are attracted by Van der Waals forces. If the repulsive forces are absent, particles agglomeration occurs. Therefore, the stability of nanoparticles dispersions can be ensured by maintaining the repulsion between the particles by different ways of stabilization.

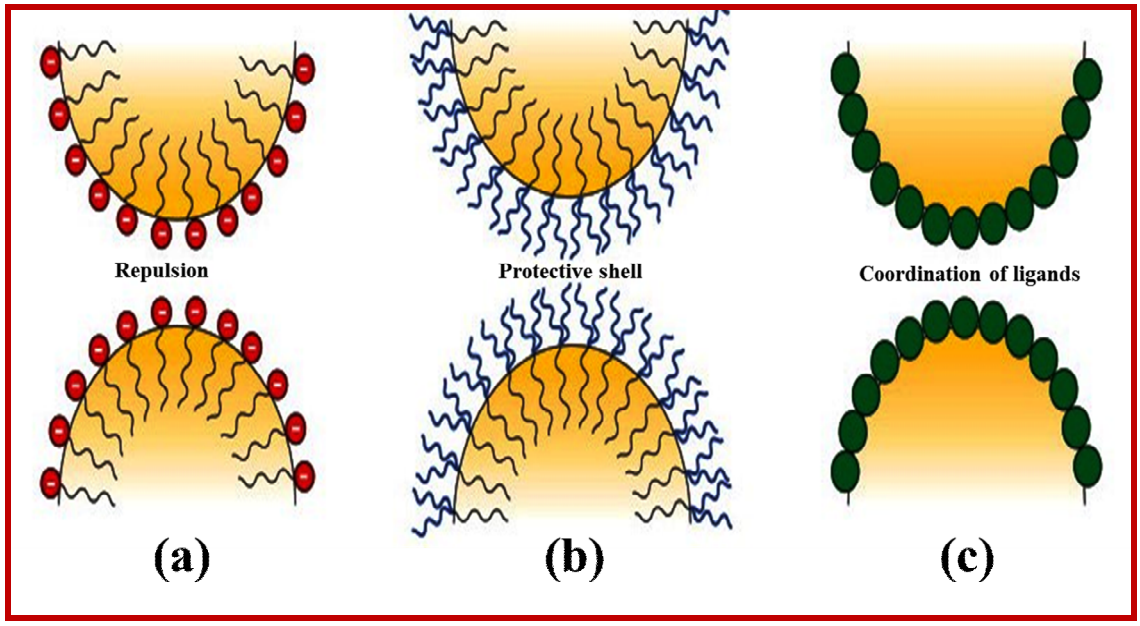

Figure 1.8 Figure represents stabilization of nanoparticles by three different ways: Electrostatic (a), Steric (b) and Ligand stabilization (c).

1.5.1 Electrostatic stabilization

Electrostatic stabilization is due to the presence of ionic compounds (halide, carboxylate, polyoxoanions, etc.) well dispersed in solution (Figure 1.8 (a)). These ions of above said ionic compounds adsorbs on to the surface of nanoparticle and generates the electrical double layer around them. This generates coulombic repulsion between the particles preventing agglomeration [Nath *et al*. (2010), Pachon *et al*. (2008), Hutter *et al.* (2004)].

1.5.2 Steric stabilization

Steric stabilization also prevents aggregation/agglomeration by introducing different stabilizers such as surfactant or polymers. These stabilizers adsorb on to the surface of nanoparticle forming a protective shell around them (Figure 1.8 (b)). When such nanoparticles approach each other, the adsorbed stabilizer macromolecules get entangled in each other. This restricts the possible microstates available to them or, in other words, it decreases the configurational entropy and thereby increases free energy of the system. Thus, such steric stabilization renders thermodynamically unstable aggregation or agglomeration. Hence, steric stabilization gives rise to well dispersed nanoparticles in sols.

1.5.3 Stabilization with ligands

Ligand stabilization occurs by coordination of metallic nanoparticles with ligands (Figure 1.8 (c)). Some of the ligands used in stabilization of nanoparticles by coordinating with their surface are phosphine, amines, thiol, oleic acid, etc. [Szpak, *et al.* (2013), Janardhanan *et al*. (2008), Yantasee *et al.* (2007), Lan *et al*. (2007)].

1.5.4 Stabilization with support material

Another method to overcome the nanoparticle agglomeration tendency is by support materials. In this process NPs are adsorbed or precipitated on large surface area, low density support materials like metal oxides such as TiO_2, ZnO, MoO_2, zeolites [Moteki *et al*. (2011)], mesoporous silica [Verho *et al.* (2014)], carbon based materials (graphite, graphene oxide, carbon nanotubes, etc. [Huang and Wang (2014), Lam and Luong (2014)]. Metal oxide support enhances activity and stability of noble metal catalysts by generating strong interaction with them. The properties of an ideal support material in terms of catalytic applications are: excellent electronic conductivity, high surface area, easy uniform dispersion of nanoparticles on support, highly corrosion resistant, strong cohesion with nanoparticles [Huang and Wang (2014), Lam and Luong (2014)]. If support materials have electron conducting nature, then it will also affect the catalysis by tuning the electron density of NPs.

1.6 Transition metal nanocatalysts

Transition metals nanoparticles and their bimetallics are widely used in many important chemical conversions such as water splitting, oxidation and reduction reactions, coupling reactions, etc. [Wu *et al.* (2017), Cao *et al.* (2016), Yue *et al*. (2015), Xu *et al.* (2015)]. These metal and bimetallic nanoparticles supported on different metal oxides and carbon based nanomaterials are also extensively used as heterogeneous catalysts in nanocatalysis. Such catalyst systems possess good adsorption properties, which allow the reactants to get adsorbed on its surface and the reaction happens on the surface of catalyst with lower activation energy. Most of reactions catalyzed by nanocatalysts proceed through Langmuir-Hinshelwood mechanism.

Among these transition metals, Au, Ag and Cu also show good visible range optical properties which can be regulated by controlling the shape and size of NPs. Interaction of these metal NPs with visible light results in the localized surface plasmon resonance (LSPR) absorbance, sensitive to the size and shape of the NPs. The dephasing of such absorbed energy, could lead to the production of energetic electrons by different modes that can drive photocatalytic transformations. These photocatalytic reactions represent a new family of chemical transformations which are electron driven photocatalytic processes different from phonon driven thermal reactions. Accordingly, the next sub-section introduces the concept of LSPR and the possible mechanisms for its utilization in achieving LSPR induced photocatalysis.

1.7 Plasmonic behaviors

When light falls on metal nanoparticles with loosely bound surface conduction electrons, it results in distortion or polarization of the surface electrons [Figure 1.9]. In case the frequency of the incident light is the same as the natural frequency of oscillation of surface conduction electrons of these nanoparticles, a resonance condition occurs, leading to localized surface plasmon resonance (LSPR) absorption [Haes *et al.* (2005), Kelly *et al.* (2003)]. Nanoparticles of Au, Ag, and Cu exhibit LSPR in the visible range, while other transition metals such as Rh etc. show LSPR in the UV regime. Since visible light is 43% of solar radiation, therefore, the applications based on visible range LSPR are preferred. The position and shape of the surface plasmon absorption (λ_{max}) of nanomaterials are strongly dependent on the size, shape, dielectric constant of the medium, and surface-adsorbed species [Jin *et al.* (2001), Link *et al.* (1999)]. Such variations in the surface-

plasmon resonance have been extensively used to study the surface phenomenon of metallic colloids [Henglein (1993)].

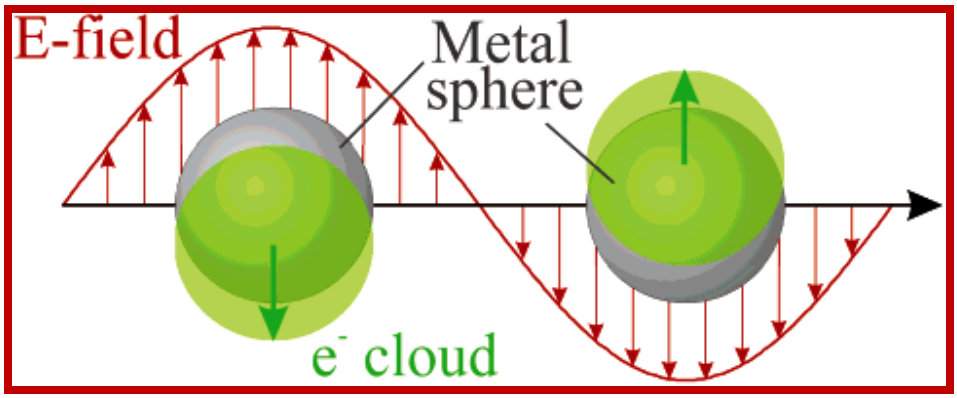

Figure 1.9 Schematic diagrams demonstrating localized surface plasmon resonance [Nath *et al.* (2010)].

Colloidal dispersion of Au, Ag and Cu NPs shows absorbance maximum in the range from 520-540 nm, 390-420 nm and 570-590 respectively [Panáček *et al.* (1996), Li *et al*. (2009)]. Mock *et al.* (2002) reported that increase in particle size red shifts the value of LSPR maximum. LSPR wavelength red shifts linearly with increase in refractive index of the medium (dielectric constant = n^2), when moved from air (n = 1.00), to water (n = 1.33), or ethanol (n = 1.36), and toluene (n = 1.50) [Gilroy *et al.* (2016)]. Hence, through theory and experiments, it is accepted that highly anisotropic nanocrystals such as nanorods, nanotriangles, and branched structures exhibits higher sensitivity with refractive index [Guo *et al*. (2015), Lee *et al*. (2006)]. Therefore, the variation in LSPR values with shape in medium of different refractive index can be represented by unit (nm/RIU). For example, Au spheres (44 nm/RIU) [Chen *et al*. (2008)], cubes (83 nm/RIU) [Chen *et al.* (2008)], rods (150-263 nm/RIU) [Khalavka *et al.* (2009)] and rattles (285 nm/RIU) [Khalavka *et al.* (2009)], complex structures of Au nanocrystals, having star (660 nm/RIU) [Nehl *et al.*

(2006)], rings (880 nm/RIU) [Larsson *et al*. (2007)] and branched structures (703 nm/RIU) [Chen *et al.* (2008)] show comparatively higher sensitivities. Noble metal nanoparticles may also exhibit more than one LSPR peaks. The number of LSPR peaks is determined by the unique ways of polarizations possible in different anisotropic nanoparticles. For a nanorod, a longitudinal and a transverse mode LSPR peaks are observed. The longitudinal mode LSPR peak occurs at longer wavelengths (polarization of free electrons along longer axis of nanorod), while the transverse mode LSPR absorbance is observed at relatively shorter wavelengths (the free electrons are polarized along shorter axis of nanorod) respectively. These two modes can be easily tuned by adjusting the aspect ratios to vary the thickness or length of nanowire [Potara *et al.* (2011), Reguera *et al.* (2017), Murphy *et al.* (2005)]. The synthesis of alloys or bimetallic compounds consist of two plasmonic metals that are capable of resonating in the visible region such as Au-Ag [Kim *et al*. (2003), Moskovits *et al.* (2002), Mallin *et al.* (2002), Link *et al.* (1999)], Au-Cu [Hajfathalian *et al.* (2015)] and Ag-Cu [Smetana *et al.* (2006)]. These may give rise to structures which demonstrate linear change in LSPR peak position with the stoichiometry of the nanocrystal. The possibility of tuning the LSPR absorbance of Au, Ag and Cu in visible region with their size, shape and composition means that these could be utilized for more specific plasmonically catalyzed reactions.

1.8 Photocatalysis

A solid which catalyzes a reaction by absorption of light is known as a photocatalyst. The acceleration of reaction in presence of photocatalyst is known as photocatalysis. The activity of photocatalyst is dependent on its ability to efficiently

generate electron-hole pair, prevent or delay recombination and finally good adsorption of the substrate on to the catalyst.

General mechanism of semiconductor photocatalysis is shown in Figure 1.10. When the semiconductor catalyst is illuminated with photon of energy equal to or greater than their band-gap energy, an electron is promoted from the valence band (VB) into the conduction band (CB), leaving a hole behind. The electron and the hole then migrate to surface of the photocatalyst. These CB electrons should have redox potentials ranging +0.5 to - 1.5 V (with respect to standard hydrogen electrode) for them to have strongly reducing tendency with respect to substrate adsorbed on the photocatalyst. Similarly, VB surface holes should range from + 1.0 to + 3.5 V (versus standard hydrogen electrode), so that they can oxidize the reactant adsorbed. Conventionally TiO_2, ZnO have extensively been used as semiconductor photocatalysts. These semiconductors have wide band gaps and therefore, require UV light for photoactivation. Ultraviolet or near-ultraviolet radiation is only 4 % in the incoming solar light spectrum on the earth [Ibhadon and Fitzpatrick (2013)]. On the other hand, the visible region ($\lambda > 400$ nm) covers 43 %, of the solar spectrum [Ibhadon and Fitzpatrick (2013)]. Hence, development of visible light driven photocatalysis is an important area of research.

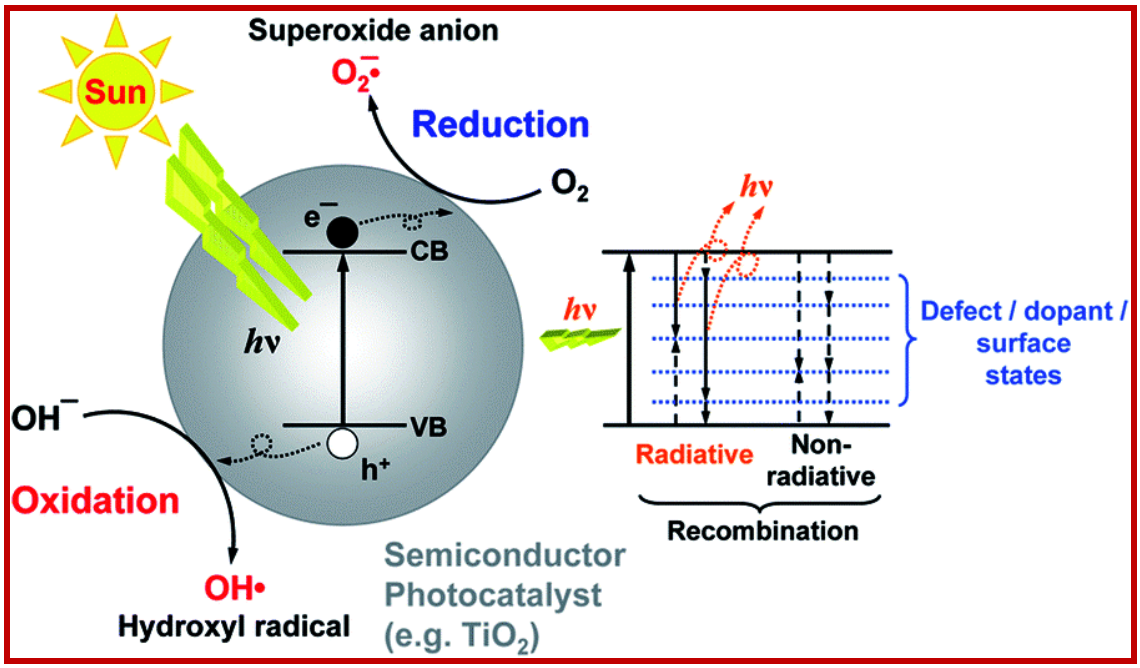

Figure 1.10 Mechanism of semiconductor photocatalysis.

1.8.1 Plasmonic photocatalysis

Recently, it has been demonstrated that strong LSPR absorbance of light in the visible range by Au, Ag and Cu (noble metals) can also be utilized for photocatalytic reactions. Such LSPR can lead to two types of photon driven chemical conversions. The dephasing of the LSPR energy absorbed by the noble metal nanoparticle results in formation of strongly concentrated electric field on the nanoparticle surface. These surface plasmons relax either by exciting electrons from the Fermi level or by re-emission of photons. The former results in what is known in literature as hot electrons. These hot electrons can be transferred to the adsorbate directly for possible photocatalysis. These light-driven, electron mediated reactions would require lower operating temperatures compared with their purely thermal counterparts [Christopher *et al.* (2010), Linic *et al.*

(2013)]. Alternatively, the re-emitted photons focused on a photoactive adsorbate can also excite electrons in it. The adsorbate can, in that case, act as possible photocatalytic centers.

In view of the focus on the catalytic and photocatalytic properties of noble metals nanoparticles in this thesis, the next few sub-sections present a brief literature survey on the catalytic applications of Au, Ag, Cu nanoparticles as well as their bimetallics.

1.9 Literature on noble metal catalysts

1.9.1 Au nanocatalysts

The first report on application of highly dispersed gold on a support material as a catalyst was on gas-phase hydrogenation of 1-butene and cyclohexene at 110 ^{0}C [Wood and Wies (1966)]. Later, Bond *et al.* (1973) efficiently applied gold supported on silica and alumina as heterogeneous catalysts for the hydrogenation of mono-olefins. Afterwards, Haruta's *et al.* (1983) demonstrated oxidation of CO to CO_2 at low temperatures (< 0 ^{0}C) in presence of oxide supported Au nanoparticles. More recent investigations have reported the effect of size and shape on the catalytic properties of Au nanoparticles. The comparative study of different nanostructures such as nanocages, nanoboxes and nanoparticles on catalytic activity was reported by Zeng *et al.* (2009). Kundu *et al.* (2009) also studied the effect of nanosphere, nanorods and nanoprisms. Size effect of Au nanoparticles on catalytic properties has also been studied [Fenger *et al.* (2012)]. Astruc (2008) explained the effect of ligands on the catalytic efficiency in the nitrophenol reduction of Au nanoparticles which are basically the electron reservoirs. The best stabilizer is concluded to be thiolate followed by citrate hence giving a low and high catalytic activity, respectively. Bimetallics of Au with Pt, Pd, Rh, Ag, Cu, etc. have also been investigated for their catalytic properties [Shah

et al. (2012)]. However, the research on catalytic properties of Au bimetallic nanoparticles is generally restricted to a few substrates. A number of reviews are available on the catalytic properties of gold [Primo *et al.* (2011)].

Investigations on plasmonic photocatalytic properties of pure Au nanoparticles loaded on insulator oxide supports have been reported in recent years. Sarina et al. (2013) observed enhancement in reductive coupling of nitrobenzene to azo compounds under ambient pressure at 40 °C when catalyzed by Au NPs supported on zirconium oxide (ZrO_2) under visible light irradiation. This is mainly because of strong LSPR absorption of visible light by Au NPs. Chen *et al.* (2008) proposed that electron excitation due to LSPR absorbance undergoes non-radiative relaxation to give rise to localized heating of the nanocatalyst surface. Thus, visible light induced heating of Au NPs surfaces on different oxide supports activate the oxidation of organic pollutants. The catalytic efficiency of Au nanoparticles loaded on supports was found to follow the order $Au/ZrO_2 > Au/CeO_2 > Au/Fe_2O_3 > Au/SiO_2$. However, as Au is expensive, researchers are increasingly paying more attention to exploration of catalytic properties of, relatively cheaper, Ag and Cu nanoparticles.

1.9.2 Silver nanocatalyst

Ag nanoparticles have also been widely synthesized and studied as catalyst in different reactions. PVP stabilized AgNPs have been used as catalyst for oxidative coupling of thiols to disulfides [Jiangmei *et al.* (2009)]. AgNPs have also been utilized as catalysts for the degradation of organic pollutants like methylene blue and chlorpyrifos [Devi *et al.* (2016)]. Different types of silver nanoparticles have been utilized for reduction of nitroarenes. Latter are extensively used as intermediates in various organic synthesis and

are also a major source of water pollution. Few examples are Poly(ethylene oxide propylphosphonamidate) (PEOPPA)-supported nanosilver [Dong *et al.* (2015)], metal-organic framework based silver nanoparticles [Moon *et al.* (2005)], semi-IPN hydrogel based silver nanoparticles [Murthy *et al.* (2008)], etc. The bimetallic nanoparticles of Ag with other metals, such as bimetallic gold/silver, core-shell nanostructures, also affect their catalytic activities [Zheng *et al.* (2013), Jiang *et al.* (2011), Huang *et al.* (2010)]. Synergistic catalytic activity is known to occur with the composition as well as the nanostructure of the bimetallic nanoparticles. Silver nanoparticles dispersed on various supports have also been used as catalysts. These include zeolite Y-dispersed silver nanoparticles [Severance and Dutta (2014)], silver/reduced graphene oxide or N-doped graphene hybrid nanocomposites [Hsu and Chen (2014), Tang *et al.* (2014)] superparamagnetic silver/halloysite nanotube/Fe_3O_4 nanocomposites [Mu et al. (2014)] silver nanoparticles supported on polymer material [Geng and Du (2014)] etc. for the reduction of 4-nitrophenol.

Recently, there has been a lot of emphasis on the plasmonic photocatalytic properties of different types of Ag nanocatalysts. Thus, core-shell nanocomposite Ag@C (i.e., Ag-C) was found to exhibit high plasmonic photocatalytic activity for the decomposition of aqueous tetraethylated rhodamine blue and gaseous acetaldehyde (CH_3CHO) under visible-light irradiation [Sun *et al*. (2009)]. Thereafter, the group of Christopher proposed the mechanism possibly being followed in direct plasmonic photocatalysis [Linic *et al.* (2013), Christopher *et al.* (2011), Christopher *et al.* (2010)]. However, the detailed study of size and shape on catalytic and plasmonic photocatalytic activity of Ag NPs is still lacking in literature.

While Ag is relatively cheaper than Au, the cost involved can still be reduced by synthesizing Ag-Cu bimetallic nanostructures with good catalytic activities prepared. Furthermore, it would be expected that such bimetallics would also exhibit good synergistic activites. That is, catalytic activities better than either of the component metals making up the bimetallic nanostructure. Therefore, the next section shall begin with details of the catalytic activities of Cu nanostructures and the subsequent sections will give a brief literature survey on the catalytic and photocatalytic properties of Ag-Cu bimetallic nanoparticulates.

1.9.3 Copper nanocatalyst

CuNPs have been widely used in click chemistry, reduction and oxidation reactions, A3 coupling, cross-coupling and multicomponent reactions, C−H functionalization, oxidative coupling, etc. [Ahmed *et al.* (2015), Acharyya *et al.* (2015), Mohan *et al.* (2015), Alves *et al.* (2015), Buckley *et al.* (2015), Nasrollahzadeh *et al.* (2015), Decan *et al.* (2014), Hu *et al.* (2014), Dakshinamoorthy *et al.* (2013)]. CuNPs are also known to be effective catalysts for hydrogenation reactions [Dragoi *et al.* (2013), Sun *et al.* (2013), Yoshida *et al.* (2010), Chen *et al.* (2010a), Kantam *et al.* (2009), Barrabes *et al.* (2006)]. Dhakshinamoorthy *et al.* (2013) have reported the synthesis of CuNPs supported on diamond NPs (DH) and their catalytic performance in the reduction of olefins with hydrazine hydrate as the reducing agent. These authors further compared the activity of Cu/DH with Au/DH and Pd/DH for the reduction of styrene to ethylbenzene. It was found that Cu/DH has higher reaction rate and conversion than the other two catalysts. Then Soomro *et al.* in 2016, reported synthesis of air stable copper nanoparticles and their use in catalysis. High reactivity of Cu NPs in cyclization of azides with terminal alkynes is

reported by Alonso *et al.* (2011). These Cu NPs have very narrow size distribution of 3 ± 1.5 nm, and therefore are very difficult to recycle. This pointed out the need of support material such as charcoal. Alonso *et al.* (2011) reported copper nanoparticles supported on charcoal (Cu NPs/C) and its application in multicomponent synthesis of 1,2,3-triazoles. Cu NPs/C proved to be an active heterogeneous catalyst and produce high yields of products in multicomponent reaction with excellent recyclability [Alonso *et al.* (2011)]. It must be mentioned here that till date there are no reports in literature on direct plasmonic activity of Cu nanoparticles.

1.9.4 Ag-Cu bimetallic catalyst

Couples of few recent reports are available on the catalytic properties of Ag-Cu bimetallic nanoparticles [Wu *et al.* (2017), Yue *et al.* (2015), Xu *et al.* (2015)]. Wu *et al.* (2017) recently reported the application of Ag-Cu nanoalloys as nanocatalysts for oxygen reduction reaction. They found that Ag-Cu bimetallic nancatalysts demonstrate activity comparable to Pt/C-20 %. Ag-Cu bimetallics have also proved to be efficient catalysts for transesterification of b-keto esters under acid/base-free condition [Yue *et al.* (2015)]. Xu *et al.* (2015) reported carbon encapsulated Ag-Cu bimetallic in nitrophenol reduction. Carbon supported Cu-Ag bimetallic was also reported as an efficient catalyst in hydroxylation of benzene to phenol [Tian *et al.* (2016)]. Only one, very recent, publication has reported that Ag-Cu bimetallic nanoparticles loaded on ZrO_2 demonstrate the visible light plasmonic enhancement of catalytic reduction of nitrobenzene to azoxybenzene [Liu *et al.* (2017)]. These authors reported change in selectivity in the reduction of nitrocompounds to the azoxy derivatives with the composition of the Ag-Cu alloy nanoparticles supported on ZrO_2 functioning.

1.9.5 Graphene as support for noble metal catalysts

Among various supports mentioned in literature, graphene and its derivatives are the most exciting recent development. However, in contrast to most supports, which are relatively inert or insulators, graphene and its derivatives posssess extraordinary physical and chemical properties. Historically, it was known quite early that oxidation of graphite gives graphite oxide. Exfoliation of the same leads to graphene oxide (GO) and finally the GO could be reduced to GO. Metal nanoparticles supported on graphene and its derivatives like graphene oxide, reduced graphene oxide and other modified graphene derivatives are also being utilized in catalysis [Hsu and Chen (2014), Tang et al. (2014), Tian et al. (2016)]. These supports not only stabilize the nanoparticle but also enhance their catalytic activity. Plasmonically excited Ag surface electrons can make transition to reduced GO, which is an excellent conductor. This leads to better charge separation and thereby increases the efficiency of the photocatalytic process. Besides this, graphene and its derivatives generally have excellent adsorption properties for organic pollutants etc. Bhunia and Jana (2014) showed that r-GO/Ag nanocomposites are good catalysts for organic pollutants under visible as well as UV light irradiation.

1.10 Model reactions for evaluation of catalytic and photocatalytic activity

The above literature survey suggests that there are only a few systematic investigations on the effect of shape, size and composition of Ag, Cu based nanocatalysts on their catalytic and plasmonic photocatalytic activities. To compare the effect of nanoparticle features on their catalytic efficacy, it is important to test their catalytic activities with respect to model reactions. Model reactions are defined in the following manner:

1. The reaction should be well controlled such that reaction between reactants A and B in presence of nanoparticles as a catalyst gives a product P without any side reaction. This reaction should not take place if nanoparticle catalyst is not present.
2. Full kinetic analysis of the reaction as a function of time and temperature should be possible, which provides a comprehensive understanding of reaction mechanism. It should be possible to measure reaction rates with high accuracy.
3. Reaction should progress under ambient conditions such as at room temperature and in mild solvents like water, etc. Under such conditions the stability of nanoparticles should be an issue.

In this thesis, two model reactions have been chosen for this purpose. One of them is the classical *p*-nitrophenol (Nip) reduction to *p*-aminophenol (AP) with $NaBH_4$ as the reducing agent. Since p-aminophenol is a well-known pharmaceutical industry intermediate requiring large scale processing, therefore, green substitute for $NaBH_4$ has also been investigated. The other one is the catalytic oxidative degradation of the sulphonated azo dye, methyl orange (MO), through an advanced oxidation protocol.

1.10.1 Nitrophenol reduction with $NaBH_4$

The reduction of Nip to AP with $NaBH_4$ serves as a model reaction for determining the kinetics and mechanism of various metal and metal oxide nanoparticles as catalysts [Aditya *et al.* (2015)]. By the use of UV-visible spectrophotometry the progress of the reaction is suitably monitored with time and hence it is a universally accepted model reaction. This reduction reaction has many environmental benefits, as Nip is converted into AP. Nip is a highly toxic organic pollutant with both carcinogenic and mutagenic effects. United States environmental protection act (USEPA) has listed it as a priority organic

pollutant [Sun *et al*. (2011)]. Nip is either a precursor or an intermediate in various industrial processes related to petrochemical manufacturing, oil refining, pesticides, insecticide, herbicide, chemical processes, synthetic dye, explosive, rubber, wood preservation operations, pulp and paper mills, paints and plastics etc. It is a stable compound due to the presence of strong electron withdrawing nitro group (NO_2) and does not get degraded in soil and ground water. Hence, it treated as an environment hazardous compound [Oturan *et al*. (2000)]. The product of reduction of Nip, p-aminophenol, is an important intermediate in the pharmaceutical industry. It also has many important industrial applications in corrosion inhibition, hair dyeing etc. [Zaharia *et al.* (2012), Patil *et al.* (2008), Dieckmann and Gray (1996)]. Considerable data is available in literature for catalytic activities of various nanoparticles. A recent review in 2016 by Gilory *et al.* has nicely summarized these developments. In this respect, effects of shape, composition and other aspects of nanostructures have neither been investigated previously nor compared with the extensive data available to understand the relative catalytic efficacy of these nanomaterials.

1.10.2 Nitrophenol reduction with glycerol

The foregoing model reaction utilizes, toxic and costly, $NaBH_4$ as the reductant. Instead of this, the use of green and renewable transfer hydrogenation agents can minimize the cost well as toxicity of the organic transformation undertaken. Since the conversion nitroarenes to aminoarenes is an industrially important class of organic transformation, therefore, there is an urgent need to explore renewable biomass derived substances which can be effective alternative transfer hydrogenation agents [Chen *et al.* (2010a), Donate (2014)]. Glycerol is a promising compound, in this respect, since it is a major byproduct of the biodiesel industries. It can also be obtained from other biomass related industrial

processes, such as during the conversion of cellulose and lignocellulose [Dutta and Pal (2014)]. Glycerol exhibits high polarity, low toxicity and flammability. It has high boiling point with an ability to form strong hydrogen bonds and to dissolve both organic and inorganic compounds [Wolfson *et al.* (2010), Gu and Jérôme (2010), Wolfson *et al.* (2009), Wolfson and Dlugy (2007)]. All these properties are necessary for its use as reducing agent as well as a solvent in synthetic chemistry. Furthermore, oxidation of glycerol in presence of catalysts results in a variety of useful products such as dihydroxyacetone, glyceraldehyde, glyceric acid, glycolic acid, hydroxypyruvic acid, oxalic acid, and tartronic acid [Tavor *et al.* (2010), Hekmat *et al.* (2003)]. Only a few reports are there in literature on transfer hydrogenation of nitroarenes to aminoarenes using green hydrogen sources like glycerol or bioethanol. These are in presence of Ru, Ni, Ir, Fe_3O_4-Ni nanocatalysts [Sudhakar *et al.* (2016), Pietrowski (2011), Maytum *et al.* (2010), Zweifel *et al.* (2008)].

1.10.3 Methyl orange oxidation

Azo dyes are basically characterized by the presence of azo groups (N=N) bound to aromatic rings are the most important class of synthetic organic dyes. Almost 50% of the commonly used synthetic dyes are azo dyes, because of their chemical stability and versatility. Methyl orange is a sulphonated azo dye having the following structure.

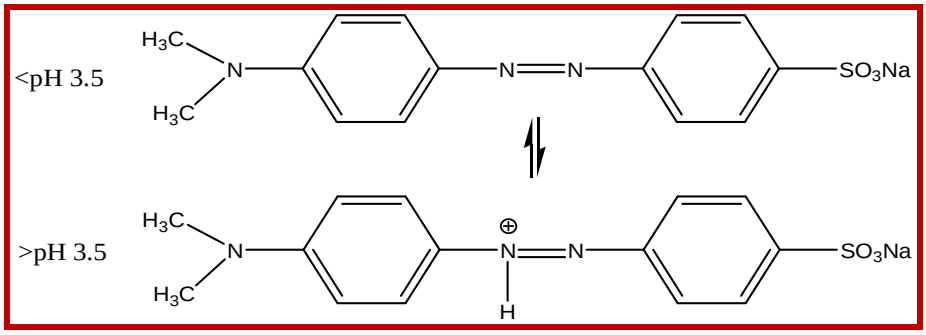

Figure 1.11 Structure of methyl orange in acidic and basic medium.

It also acts as pH indicator, shows red color in acidic medium and yellow color in basic medium. It was revealed that majority of industrial dyes are sulphonated azo dyes. Degradation products of sulphonated dyes gives two major products due to cleavage of (N = N) bond. The sulphonated and unsulphonated aromatic amines produced are toxic and carcinogenic. Therefore, complete mineralization of such azo dyes into CO_2 and water is necessary to reduce the toxicity in the environment.

Methyl orange (MO) has been widely used as a model pollutant dye for evaluating Fenton like oxidative degradation activities of various catalysts. However, a thorough literature survey shows that there are no reports on use of nanoparticles of Ag, Cu or their bimetallics as catalysts for oxidative degradation of MO.

1.11 Aim of the thesis

The foregoing literature survey shows that there are only a few studies on the effect of shape, size and composition of the nanoparticles on their catalytic properties. There have been few systematic investigations on the effect of size and shape of Au nanoparticles on their catalytic properties. Therefore, this thesis deals with the synthesis and catalytic applications of monometallic and bimetallic Ag, Cu NPs. Then reduced graphene oxide supported Ag, Cu, Ag-Cu bimetallic nanoparticles are prepared, characterized and their catalytic properties evaluated.

The catalytic activities of the nanomaterials prepared in the thesis are investigated with respect to i) model *p*-nitrophenol reduction to *p*-aminophenol with $NaBH_4$ as the reducing agent, ii) *p*-nitrophenol reduction to *p*-aminophenol with glycerol as the green

hydrogen source and iii) the model oxidative degradation of the sulphonated azo dye, methyl orange (MO), through advanced oxidation protocol. The pointwise objectives of this thesis are enumerated below.

1) Synthesis and characterization of PVP stabilized Ag nanoparticles with varying fractions of anisotropically shaped nanostructures. Investigation of the effect of such varying percentages of anisotropically shaped nanoparticles on their catalytic and plasmonic photocatalytic properties.
2) Synthesis and characterization of curcumin stabilized Ag nanoparticles. Evaluation of the effect of amount of curcumin functionalization of Ag nanoparticles on their catalytic and plasmonic photocatalytic properties. Curcumin, being a molecule with its HOMO-LUMO gap in visible range is expected to enhance photocatalytic activity of Ag nanoparticles.
3) Preparation and characterization of PVP stabilized copper nanoparticles of two sizes. Studies on effect of size of copper nanoparticles on their catalytic and plasmonic photocatalytic properties.
4) Preparation and characterization of different types of Ag-Cu bimetallic nanostructures. Effect of different types of nanostructures (phase separated, core-shell etc.) on their catalytic and plasmonic photocatalytic properties.
5) Synthesis and characterization of Ag, Cu and their bimetallics on reduced graphene oxide (rGO) support. Investigations on their catalytic and plasmonic photocatalytic properties.